



Statistical Analysis of the Inhibition of Carbon Steel Corrosion in 3.5 wt.% NaCl Solution Using Lawsonia Extract

Ashraf M. El-Shamy¹, Medhat A. El-Hadek², Ahmed E. Nassef², Reham A. El-Bindary^{2*}

Received: 18 July 2020; Accepted: 28 September 2020

ABSTRACT

The corrosion performance of carbon steel after wide-ranging acquaintance load of aqueous extract of Lawsonia inermis (LI) as a green inhibitor in saline media was inspected. These studies have been supported by means of open-circuit potential (OCP), potentiodynamic polarization technique (PD) and electrochemical impedance spectroscopy (EIS). In addition, the scanning electron microscopy (SEM) and energy-dispersive X-ray (EDX) analysis stayed applied as a complementary tool for surface characterization. For more illustration theoretical and statistical studies were subjected for corrosion inhibition efficiency. All results inveterate that, the carbon steel alloy corrosion rate decreases with the upsurge of inhibitor concentration and LI are an important deterrent for the saline solutions to corrosion of carbon steel alloy. The presence of LI particles anywhere decreased the cathodic, anodic and corrosion currents and the rate of deterioration, as well as improved polarization and solvent resistance of carbon steel alloy in the saline electrolyte. Statistical tests using the Box–Behnken process stayed used to observe the effect of principal parameters (i.e., concentration of inhibitors, temperature, and speed of rotation) on the effectiveness of inhibition and corrosion level of carbon steel alloy.

Keywords: Saline solutions; Green corrosion inhibitor; carbon steel alloy; Electrochemical techniques.

1. INTRODUCTION

Various metallic structure manufacturing activities include the application of corrosion inhibitors to waters to regulate the corrosion rate [1] [2] [3]. The corrosion inhibitors for carbon steel surfaces are predominantly authoritative concerning the manufacturing towards the saline actions of the surrounding environment [4] [5]. Saltwater is exploited in the cooling systems and in many cases is also used for injection in petroleum wells to enhance their productivity. However, these conditions on carbon steel pipelines are considered highly corrosive. Within the saline medium, minor discussions with the corrosion inhibition occur [6]. Frequently, operative organic compounds act as corrosion inhibitors constitute in its molecular assembly nitrogen, sulfur, or oxygen atoms as well as electronegative groups and π -bonds [7] [8]. The hindering consequence of these organic composites is contingent with the adsorption process which associated

amongst the metallic surface and its inhibitor molecules [9] [10] [11]. By this means, the projected mode of action of the corrosion inhibition efficacy may be done via electrostatic forces of van der Waals amongst the active metals and the charged particles of the corrosion inhibitor. It is clearly known that, the vacant d-orbitals of steel which joining with the free electrons in the electronegative atoms which exist in the inhibitor particles, or maybe combined with these approaches [12] [13] [14]. Innumerable explorations were directed to measure some naturally extracts of some ingredients as green inhibitor of corrosion for several metallic structures in numerous situations [15] [16] [17]. The aqueous extract from various natural products may be used as a healthy and green inhibitor of corrosion [18] [19]. The aqueous extract consists of numerous types of organic compounds which act in synergistic action to protect metals from corrosion in severe environments [20] [21]. Some natural products exist in a linear biopolymer type, in which the amino acids are the monomer units which joined to each other's through the connecting amongst (-NH₂) group of each amino acid by means of a carboxylic acid group (-COOH) of other amino acids in other name peptide bonds. Subsequently, these bonds contain many monomers connected and the side chains contain an alkyl group were described [22] [23]. In all-purpose, the functional groups as an amine group (-NH₂) and carboxyl group (-COOH), attached and or adsorbed to the metal surface and are protected from severe environmental conditions. Hence, the organic structures of

¹ Department of Physical Chemistry, Electrochemistry and Corrosion Lab, National Research Centre, El-Bohouth St. 33, Dokki, PO 12622, Giza, Egypt

² Department of Production and Mechanical Design Engineering, Faculty of Engineering, Port-Said University, Port-Fouad, Egypt

*Corresponding author: E-mail address: ra.bindary@yahoo.com

aqueous extract comprised elements such as (C), (H), (O), and (N), in addition some extra elements may be exist in the crosswise branches [24] [25]. By this way, the aqueous extract from natural products might be applicant to usage as inhibitors. In addition, the aqueous extracts from natural products are ecofriendly, low-cost, punctually available and regenerative constituents. The goal of this study is to explore the possibility of using the aqueous extract of *Lawsonia inermis* as a green composite for the corrosion of carbon steel at 3.5 wt.% NaCl, employing OCP, PD and EIS. These methods were applied to investigate the effect of flow rate, temperature and loads of inhibitor on the rate of carbon steel corrosion. The optimal conditions amongst the variable parameters influencing the levels of corrosion and inhibition efficiency improvements were measured using research arithmetic enterprise (Box–Behnken). This work was also undertaken to find a naturally occurring, cheap, and environmentally safe substance that which could be used to inhibit corrosion of carbon steel. The use of such substances shall at the same time establish the objectives on the economy and the environment.

2. RESOURCES AND PROCEDURES

2.1. Resources

Pure sodium chloride (NaCl, Merck, 96%), *Lawsonia inermis* powder, acetone (C₃H₆O, Merck, 99.0%) and ethanol (C₂H₅OH, Merck, 99.9%) stayed applied by way of customary. The carbon steel alloy substrate through a quadrangular form with superficial proportions of 1x1 cm was labouring for the electrochemical assessments.

2.2. Carbon Steel Alloy

The extract of *Lawsonia inermis* (LI) inhibition belongings stayed investigated on the carbon steel alloy of electrode with the form of flag and surface dimensions of (1×1 cm²). The XRF shows the chemical conformation of the working carbon steel alloy and the constituents are: 0.047% C, 0.003% Al, 0.037% Si, 0.017% P, 0.013% S, 0.02% Ti, 0.049% Cr, 0.29% Mn, 0.057% Ni, 0.054% Cu, 0.002% Mo, 0.002% Sn and the balance Fe, was used in this study. The equivalent carbon content of the carbon steel alloy was calculated and found to be 0.119 [26]. The processed sample was washed away with bi-distilled water, and dried out earlier. NaCl and bi-distilled water were fitted with the damaging 3.5 wt.% NaCl solutions shielded by LI at many other concentrations [11].

2.3. Preparation of *Lawsonia inermis* Extract

Lawsonia inermis extract (LI) was obtained by dispersing 100 g/500 mL of *Lawsonia inermis* compound distilled water in 1000 ml volumetric flask, boiling for 30 min, gradually filtering, and concentrating the filtrate to 100 mL.

The subsequent solution was then used in electrochemical experiments for preparation of the test electrolytes [27].

2.4. Electrochemical measurements

The electrochemical inquiries were supposed to apply in a tube-shaped Pyrex glass cell, using a conservative three electrodes. The steel of carbon electrodes with a 1 cm² visible area were employed as a working electrode. The Ag/AgCl and platinum electrode were operated as a reference and auxiliary electrode, individually. The electrochemical experiments stayed performed using a traditional cylindrical glass cell with three electrodes at a temperature of 25 °C. The working electrode was carbon steel with an area of 1 cm² above and the rest was covered by the commercial use of epoxy resin. The electrode was before each experiment permitted to rust spontaneously and reported its open-circuit potential (OCP) as a meaning of time active to 30.0 min. A steady-state potential was obtained at this time, i.e. the E_{corr} of the operating electrode. The electrochemical tests were used meticulously by Volta-Master 4 software on the Volta-Lab PGZ402 potentiostat. Before conducting the electrochemical inquiries, the carbon steel electrodes were engrossed in a 3.5 wt.% NaCl solution with and without various inhibitor masses for 30 min to maintain a steady state open circuit (E_{ocp}) potential. Potentiodynamic polarization values were generated by scanning the potential for forward position at a scan rate of 0.001 V/s from -1.0 to -0.2 V vs. Ag/AgCl. In this study we are using a 10 mV amplitude disturbance signal for both 2 and 5 Hz oscillation frequencies. The electrochemical impedance AC indications of 10 mV amplitude peak-to-peak in the occurrence variety of 100 kHz to 5 mHz were used for explanations. The impedance descriptions are given in the expression of the Nyquist and Bode. Anodic and cathodic in the end Polarization curves were collected by a scanning rate of 1 mV/s separately since -0.7 to 0.7 V. For each concentration of inhibitor, the above processes have been repeated. In addition, the (EIS) tests were conducted utilizing AC signal between both the desired frequency limit of 100 kHz and the minimum intensity limit of 0.03 Hz at open-circuit potential with a 10 mV frequency. The amplitude data was collected and equipped with the ZSimpWin 3.60 simulator, comparable circuit program [12] [23]. Be noticed that the corrosion inhibitor is added to the saline solution before immersion of the electrode to a sure that the homogeneous dispersion of inhibitor in the solution before subjected the electrode into the electrolyte.

2.5. SEM and EDX investigations

The superficial test of steel carbon alloy was surveyed by scanning electron microscope (SEM) investigation at fast-

tracking voltage of 20 kV (JEOL-JSM-6510 LV). The molecular dispersal of carbon steel alloy was scrutinized using the harmonizing method of (EDX) and taken on a Leo1430VP microscope with employed voltage 5 kV [28].

2.6. Statistical Evaluation

Box–Behnken study approach to test the inhibition performance and corrosion rate of carbon steel alloy using **LI** by means of an inhibitor [29] [30] aimed at the factors (rotation speed, temperature and concentration of inhibitor) is exposed in Table 1. The answer factors stayed established using simplistic diagrams of the rejoinder designs and the largest analytical imitations. The Box–Behnken innovativeness can acceptable the succeeding prototypical method [31]:

$$E(y) = \beta_0 \sum_{i=1}^3 \beta_i X_i + \sum_{i=1}^3 \sum_{j=1}^3 \beta_{ij} X_i X_j \quad (1)$$

where y is the answer adaptable approximation, X_i 's are the independent limitations (rotation speed, inhibitor load and temperature) that are documented for every new run, and β_0 , β_i , and β_{ij} are the deteriorating restrictions. DesignExpert 6.1, Software bundle, Stat–Ease, Minneapolis, USA, was castoff for the deterioration of investigative statistics and the superficial project of response. Approximate variance analysis (ANOVA) was used for the statistical parameters. The sum of the investigational implications relevant for the polynomial typical calculation was expressed to evaluate the coefficient, R^2 .

3. RESULTS AND DISCUSSION

3.1. Open-circuit potential

The corrosion efficiency of carbon steel alloy and the penetrability of the superficial layer can be preserved by open-circuit potential (OCP) measurements [32]. Fig. 1 shows the time-dependent disparity of OCP of carbon steel alloy occupied in 3.5 wt.% NaCl solutions with various **LI** inhibitor concentrations. The OCP values were noticed to be lifted in a positive way. It explains that in the event of the **LI** inhibitor, the kinetics of the anodic reaction of carbon steel was more strappingly predisposed in 3.5 wt.% NaCl solutions. This performance is signifying that, the development and creation of a protective film due to the inhibitor adsorption particles on the metallic superficial. This action remains more proved by decreasing the active sites of the superficial of carbon steel. However, the shift in OCP values between the presence and absence of the inhibitor depends on the **LI** inhibitor concentration, which indicates that the inhibitor investigated is a different receptor inhibitor [33].

Table 1: Corrosion amount and inhibition efficacy of carbon steel alloy in 3.5 wt.% NaCl solution at pressure (101325 Pa) and time (1200 s).

Run	Inhibit or conc. (%)	Rotation speed (rpm)	Temp. (°C)	Corrosion Rate (mL/Y)	Inhibition Efficacy (%)
1	5	150	50	38.2	43.74
2	10	150	50	8.9	86.89
3	5	250	50	42.1	42.95
4	10	250	50	11.9	83.87
5	5	200	25	28.6	48.18
6	10	200	25	7.8	85.86
7	5	200	75	53.8	37.36
8	10	200	75	21.6	74.85
9	7.5	150	25	10.12	81.22
10	7.5	250	25	13.14	77.31
11	7.5	150	75	17.63	67.29
12	7.5	250	75	20.39	64.78
13	7.5	200	50	13.33	75.85
14	7.5	200	50	13.33	75.85
15	7.5	200	50	13.33	75.85
16	7.5	200	50	13.33	75.85
17	7.5	200	50	13.33	75.85

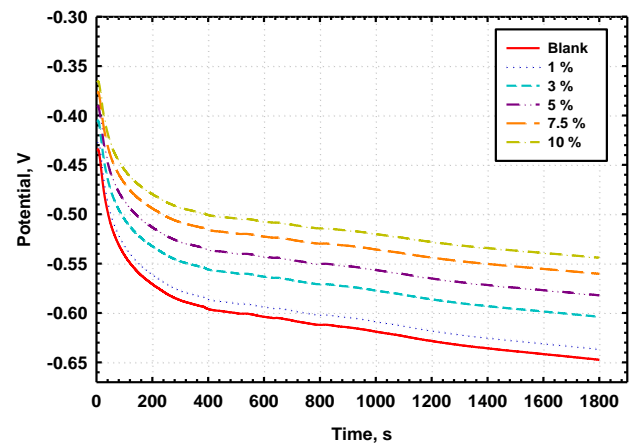


Figure 1: Open-circuit potential vs. time of carbon steel alloy taster occupied in 3.5 wt.% NaCl media and various LI loads.

3.2. Potentiodynamic polarization measurements

These trials were supported to identify the outcome of time on the decomposition performance of the carbon steel alloy in the saline electrolytes. Fig. 2 shows that the curves of potentiodynamic polarization gained for carbon steel after 30 min in 3.5 wt.% NaCl solution with various **LI** concentrations. The corrosion potential (E_{corr}) values, the density of corrosion current (I_{corr}) and the inhibition efficacy (η), the cathodic (β_c) and the anodic (β_a) Tafel slope were recorded in Table 2. These values were calculated as per the subsequent formula [34]:

$$\eta_{Tafel}(\%) = \frac{I_{corr} - I_{corr(i)}}{I_{corr}} \times 100 \quad (2)$$

Wherever (I_{corr}) and ($I_{corr(i)}$) are the densities of corrosion current for carbon steel electrode in the un-injected and injected electrolytes, individually.

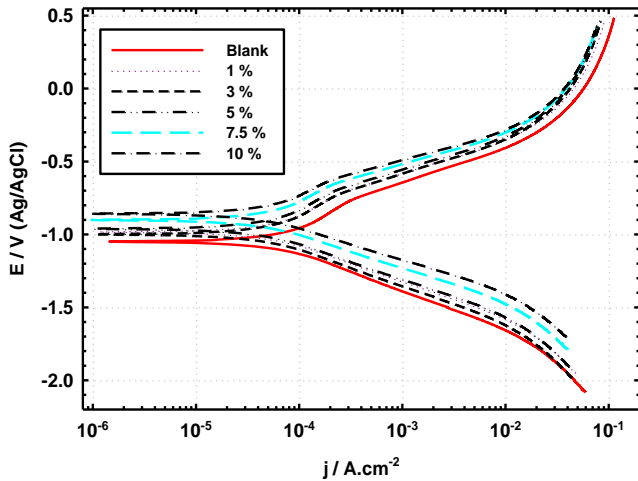
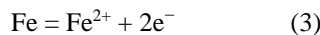


Figure 2: Potentiodynamic polarization models of carbon steel alloy sample absorbed in salt solution and varied LI loads

The addition of **LI** inhibitor molecules saline solution causes an extraordinary reduction in the density of corrosion current (I_{corr}) in all the concentration of inhibitor associated to the blank experiment. The anodic reaction is well recognized as the dissolution of carbon steel, which devours the produced electrons at the cathode, see Eq. (3) [35]:



Although, the reaction of carbon steel at cathodic, that devours the produced electrons. The reaction at the anodic in 3.5 wt.% NaCl electrolytes is concerned with the evolution of hydrogen conferring to the subsequent Eq. (4):

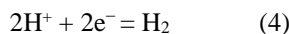
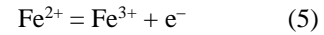


Table 2. The corrosion limits obtained from the results of potentialodynamic polarization for the carbon steel alloy superficial embedded in 3.5 wt.% NaCl solutions for dissimilar concentrations of LI.

Medium	Parameters						
	$-B_c$ mV/dec	E_{corr} mV	j_{corr} μAcm^{-2}	B_a mV/dec	R_p Ωcm^2	R_{corr} Mm/y	$I.E$ %
Absolute	141.18	645	3304	83.7	4.58	57.9	–
1 %	139.21	636	3257	82.53	4.51	43.6	24.69
3 %	131.77	602	3082	78.11	4.26	34.9	39.72
5 %	126.74	579	2964	75.12	4.1	29.2	49.56
7.5 %	122.36	559	2861	72.51	3.96	19.7	65.75
10 %	119.3	545	2789	70.69	3.86	8.3	85.66

Noticeably that, growing the time shifts the E_{Corr} near to a reduced amount of the negative data, upsurges the deterioration of the carbon steel alloy over growing the results of j_{corr} and R_{corr} and lessening the equivalent R_p results. Because of growing the time upsurges the deterioration of the carbon steel through the decomposition under the nonstop outbreak of sodium chloride to the superficial, since does not permit the surface to build the oxide film and/or rust which decreased the deterioration process [35]. Additional purpose is the ferrous ions (Fe^{2+}) remain unchanging and oxidized to ferric ions (Fe^{3+}) by way of mentioned in the following equation:



The brutality of this reaction upsurges with growing the time of immersion, since it could prime to the augmented corrosion of carbon steel alloy and clarify the amplified currents and the rate of corrosion with growing the periods of time. Growing the functional potential in fewer negative paths additional simplifies.

3.3. Measurements for Electrical Impedance Spectroscopy (EIS)

The EIS technique was exploited by evaluating the inhibition function in additional dimension. Fig. 3 demonstrations the assimilated Nyquist diagrams of carbon steel in 3.5 wt.% NaCl intermediate without and with several amounts of **LI**. The Nyquist figure, of carbon steel with and without the consequence of **LI**, is represented by capacitive one multipart at higher frequency (HF) per a slight inductive trial at little frequency data (LF) [36]. At field with high frequencies, the capacitive circle (charge transfer) can be identified while the inductive circle next to

the lower frequencies area is certified to reduce the absorbed optimal structures monitoring the anodic mode of action [37] [38]. Evidently, the diameters of capacitive circlets (Fig. 3) increase with the development in **LI** percentage, proves that, the upsurge of charge transfer obstruction besides advancement of the inhibition effect on carbon steel weathering [39]. The evidence that the production of **LI** to 3.5 wt.% NaCl solutions increases the resistance of load transfer by forming a protective layer on the surface of the carbon steel alloy incapable of modifying different characteristics of the recital. Alike consequences using the polarization verified that described **LI** adding does not alter the electrochemical reaction mode. The impedance of Nyquist designs of carbon steel alloy in 3.5 wt.% sodium chloride solutions comprising **LI** were categorized by appropriate the investigational results to progress the suitable physically model and abstract the limitations that describe the rust development. The similar circuit modally applied to accept the investigational results of impedance were $[R_s (Q_{R_{ct}})]$, which comprise solution resistance (R_s), the element of phase constant (Q), resistance of charge transfer (R_{ct}). The results of R_{ct} will be premeditated by the next Eq. (6) [39]:

$$R_{ct} = Z_r(\text{At low } f) - Z_r(\text{At high } f) \quad (6)$$

Where $Z_r(\text{at low } f)$ and $Z_r(\text{at high } f)$ are, correspondingly low and high frequency impedance. Great performance of double layer technologies (C_{dl}) were replaced via a continuous point element (CPE) in the corresponding circuit's classical. Avoid the nonconformity consequential beginning the occurrence spreading, which ascribed towards irregularity and in consistencies of the compacted superficial and Eq. (7) shows the impedance of the CPE [40]:

$$Z_{CPE} = \frac{1}{Y_o(j\omega)^n} \quad (7)$$

where Y_o stays the degree of CPE ($\Omega^{-1} \text{ s}^n \text{ cm}^{-2}$), j stays the imaginary source, and ω stays the sine wave variation of angular regularity (in rad s^{-1}), $j^2 = -1$ is the fantasy root besides n is an experiential proponent ($0.0 \leq n \leq 1.0$) might dealings the nonconformity after the perfect capacitive performance. Since the principles of correlated reserve efficiencies, η_z (%), were identified and recorded in Table 3, rendering to the ensuing eq. (8):

$$\eta_z(\%) = \frac{R_{ct(i)} - R_{ct}}{R_{ct(i)}} \times 100 \quad (8)$$

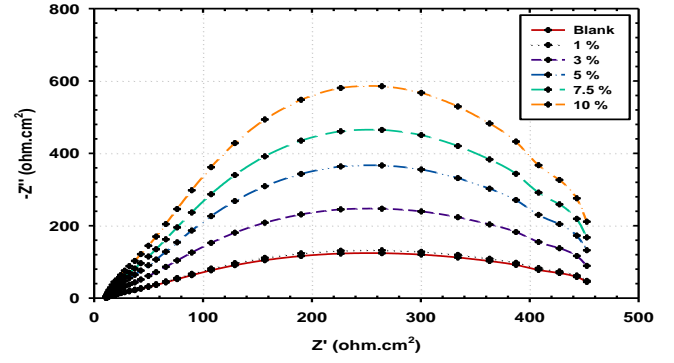


Figure 3: Nyquist carbon steel alloy sample plots dissolved in 3.5 wt.% NaCl electrolyte and different LI masses

Table 3. The gained limits through appropriate the EIS data through the corresponding route publicized trendy (Fig. 4) for carbon steel alloy in 3.5 wt.% NaCl solution.

Medium %	Parameters						
	$R_s/\Omega \text{ cm}^2$	$Y_o/F \text{ cm}^2$	n	$R_{p1}/\Omega \text{ cm}^2$	$R_{p2}/\Omega \text{ cm}^2$	L/H	I.E, %
Blank	2.445	2.1×10^{-4}	126.14	10.667	4.892	29.632	-
1	2.584	2.0×10^{-4}	1.504	15.255	7.268	30.616	43.01
3	3.124	1.8×10^{-4}	1.499	22.806	9.419	32.484	58.72
5	3.993	1.8×10^{-4}	1.579	33.613	12.972	35.824	68.57
7.5	5.091	1.5×10^{-4}	1.529	41.201	15.375	38.123	84.15
10	4.957	1.1×10^{-4}	1.358	47.936	16.142	36.010	94.23

wherever (R_{ct}) and ($R_{ct(i)}$) remain the resistance of charge-transfer standards in nonappearance and existing **LI**. It's originated that η_z (%) upsurges with the **LI** loads. Conversely, it seems in Bode plots that, the adding of **LI** to 3.5 wt.% NaCl solutions consequences in an upsurge in the impedance model which additional rises with growing unconfined **LI** loads (Fig. 3). It can be ascribed to the development of a protecting flick of the **LI** fragments on the surface of steel electrodes which hinders the dissolution of carbon steel alloy. After steady state potential after 30 min of immersion the corrosion of carbon steel in 3.5 wt.% NaCl in the attendance of studied plant extract was investigated at 30 °C by EIS method. Nyquist and Bode schemes are used in the nonappearance and inclusion of the extract examined in Figs. 3 and 4, correspondingly. Evidently all Nyquist plots display a single capacitive circuit, both in uninhibited and inhibit solutions. The analogous circuit layout Fig. 4 which involves the R_s or R solution resistance and the C_{dl} binary layer capacitance which stands put in parallel with the R_{ct} load assignment

resistance owing to the transfer load response. The higher (R_{ct}) values are generally associated with a slower system of corroding. As exposed in Fig. 4, it is a solitary continual time for the deterioration procedure at the steel-electrolyte boundary in the designs of the phase angle. The upsurge in the heights of the peak with rising magnitudes of **LI** suggests an extra capacitive rejoinder at the steel-electrolyte border since, the adsorption of **LI** fragments and henceforth added embarrassment stimulus. EIS data likewise approve the inhibiting recital of **LI**, which depiction the similar tendency as individuals increased from the potentiodynamic polarization approaches.

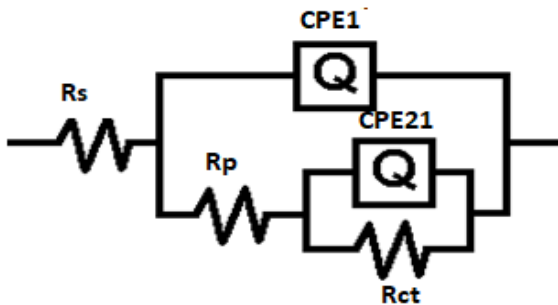


Figure 4: The model carbon steel sample equivalent circuit in 3.5 wt.% NaCl electrolyte besides various **LI** masses.

3.4. Electron microscopy (SEM) scanning and energy-dispersive X-ray (EDX) research

Fig. 5 shows the SEM image of carbon steel alloy superficial subsequently flooded in 3.5 wt.% NaCl in absence and presence of 10% **LI** inhibitor. Here is the development of corrosion crops that seemingly shelters the entire superficial of carbon steel alloy. The corrosion crops formerly arrangement a penetrable deposit that does not allow for the defense of carbon steel, furthermore shows the EDX spectra for the carbon steel after exposure to 3.5 wt.% NaCl lacking inhibitor. It was well seen that in saline medium the EDX spectrum demonstrates the reflective peaks of many elements restricted in the electrode surface's chemical configuration. Alternatively, the application of the **LI** inhibitor to the damaging electrolyte greatly reduced the corrosion rate of carbon steel alloy as present in the SEM picture (Fig. 5). This henceforth prevents the production of corrosion products which lead to the deterioration of the surface carbon steel. In addition, the EDX graph (Fig. 6) reveals that, in the chemical configuration of the **LI** inhibitor, the presence of **LI** inhibitor primes at the entrance of the distinguishing peak of oxygen and carbon. In addition, compared to uninhibited carbon steel alloy surface testing, the Fe peaks are substantially repressed. Such Fe showings occur because the inhibitor film is superimposed on the metal substrate [41]. In Fig. 6, the EDX results showed the (N) element in the presence of **LI**, which prove that the inhibitor form a protective layer on the electrode surface in Fig. 6A, while it is not detected in absence of **LI** (Fig. 6B), this results prove that the source of nitrogen element is the corrosion inhibitor. In addition, the surface roughness is clearly noticed in absence and in the presence of the corrosion inhibitor and it is clearly noticed that, the

presence of 10 % of the corrosion inhibitor is the best formed surface regarding to the surface roughness.

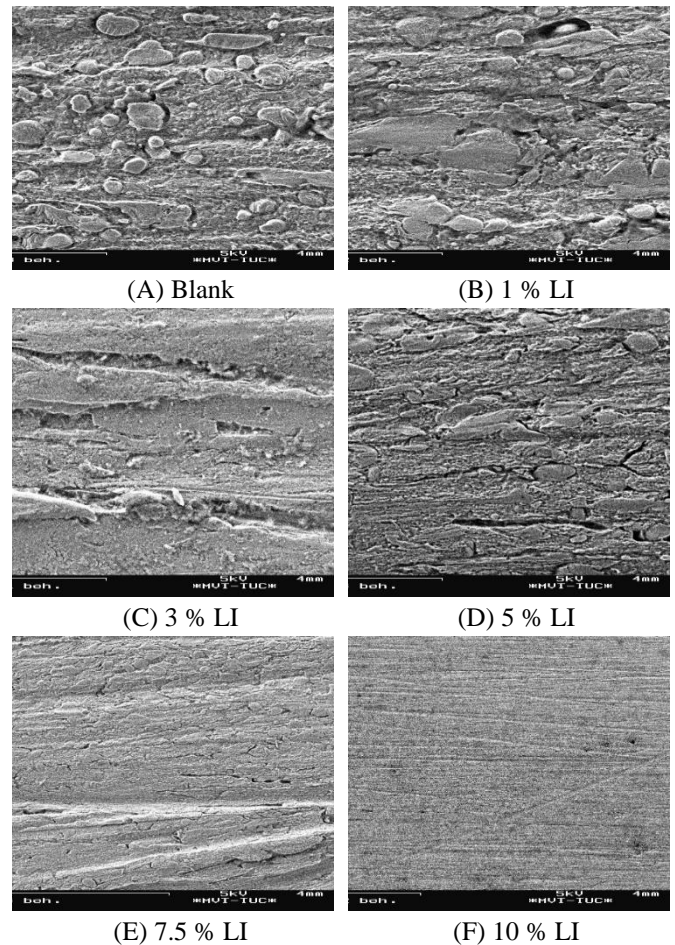


Figure 5: SEM images of the carbon steel surfaces film formed on microelectrodes in 3.5 wt.% NaCl (A) without **LI** and (B), (C), (D), (E) and (F) with 1, 3, 5, 7.5 and 10 % **LI**, individually

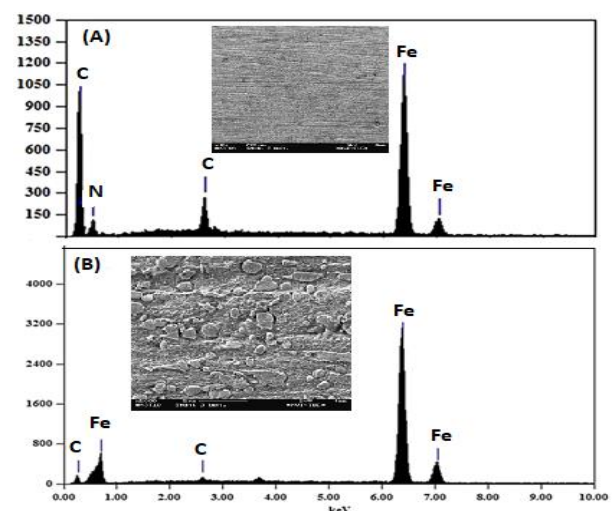


Figure 6: EDX diagram of the carbon steel surfaces in 3.5 wt.% NaCl: (A) by 10% **LI** besides, (B) in absence of **LI**, individually

3.5. Statistical Assessment

3.5.1. Experimental conditions optimization

The Box–Behnken design included a whole of 17 investigational runs to maximize the three individual factors (rotation speed, inhibitor concentration, and temperature) (Table 1).

3.5.2. Rate of corrosion

Fig. 7 displays the contour design of the effect of rotational speed and inhibitor concentration proceeding carbon steel alloy corrosion at dissimilar temperatures of 25, 50 and 75 °C. At 25°C the corrosion rate reduced by 24.33 to 8.75 % despite an increased concentration of inhibitors from 5 to 10 %. Similarly, by increasing rotational speed since 150 to 250 rpm, indicating no response. Growing the temperature to 50.0 and/or 75.0 °C increases the risk of corrosion with can inhibitor concentration and marginal effect with rotational velocity.

The contour plot resulting from the temperature and concentration of inhibitors on the corrosion degree of carbon steel alloy by rotational speeds of 150, 200 and 250 rpm revealed that the corrosion rate decreased from 29.93 to 8.36% at 150 rpm with rising inhibitor adsorption from 5.0 to 10.0%. Growing temperature from 25.0 to 75.0 °C often increases the degree of corrosion from 11.14 to 15.26 %, which means no impact. As the rotation haste increases to 200.0 and/or 250.0 rpm, the corrosion degree increased by an increase temperature and concentration of the inhibitor.

The contour plot resulting from rotational haste besides temperature arranged the carbon steel corrosion rate at various adsorptions of inhibitor 5.0, 7.5 and 10.0% revealed that by 5.0% the rate of corrosion decreased since 50.68 towards 33.51% by increasing rotational speed between 150–250 rpm. Increasing the concentration of inhibitors from 5 to 10% also lowers the corrosion rate from 39.07 to 12.09%. By changing the amount of inhibitors to 7.5 and/or 10 %, the rate of corrosion increases with increasing rotation speed and temperature.

Image of Fig. 8 Shows a 3D plot of carbon steel alloy corrosion rate by means of a variable of inhibitor adsorption besides velocity of rotation by various temperatures 25.0, 50.0 and 75.0 °C. It reveals that the extreme corrosion degree was 33.97 mL/Y at 25 °C. The temperature change since 50.0 towards 75.0 °C also raises the average corrosion degree to 41.14 and 52.98 mL/Y, individually.

The 3D scheme of the effect of inhibitor mass and temperature on carbon steel alloy's probability of failure at different rotational speeds of 150, 200 and 250 rpm revealed that the high corrosion rate was 49.49 mL/Y at 150 rpm. Similarly, increasing the rotation haste since 200.0

towards 250.0 displays irrelevant increases the maximum corrosion degree to 51.58 and 52.98 mL/ Y, individually.

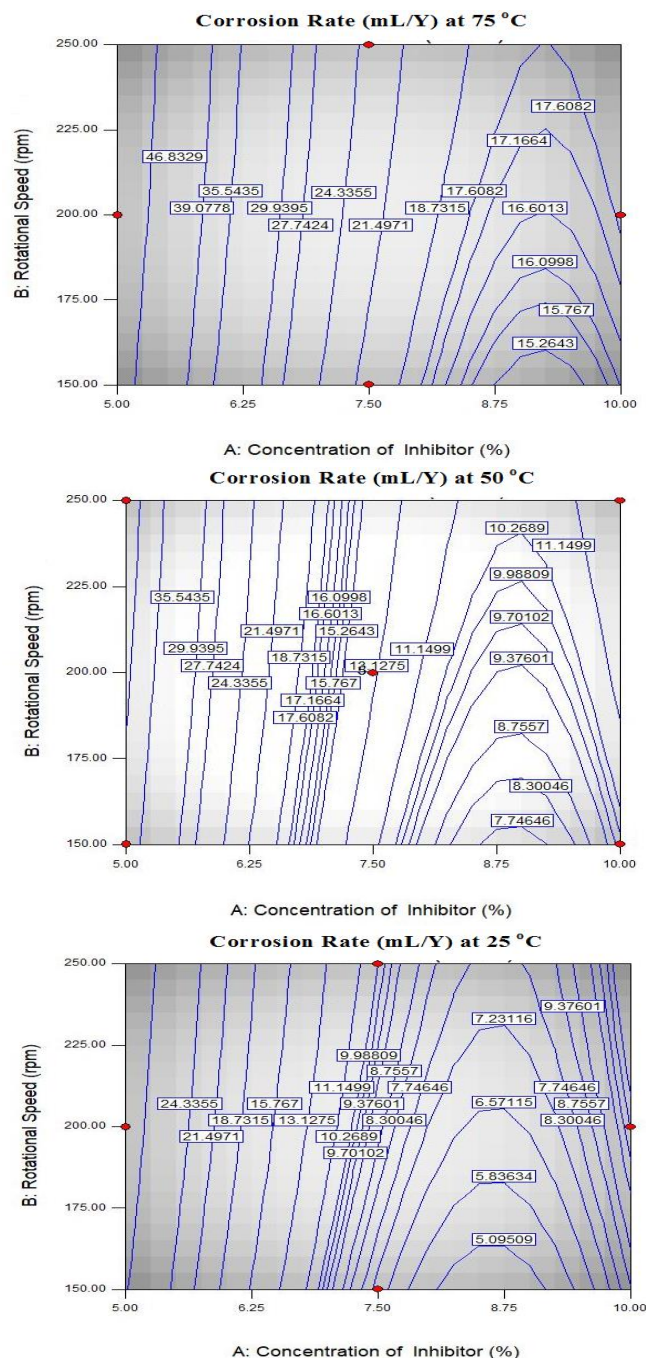


Figure 7: Contour plot of corrosion rate at temperatures 25, 50 and 75 °C as inhibitor load and rotational speed.

As just a meaning of temperature and rotation speed at dissimilar inhibitor adsorption 5.0, 7.5 and 10.0 %, the 3D scheme of carbon steel alloy corrosion degree revealed that the high corrosion rate was 52.98 mL / Y at 5%. Increasing the concentration of inhibitors from 7.5 to

10% also lowers the extreme corrosion degree to 23.56 besides 18.71 mL/Y, individually.

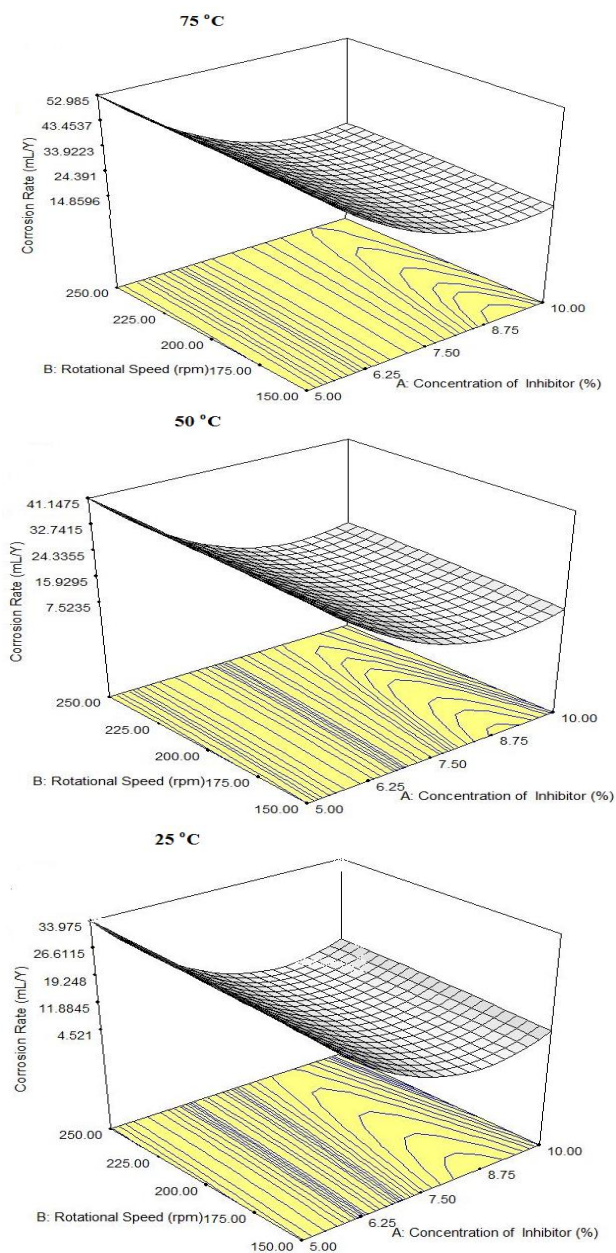


Figure 8: 3D corrosion degree plot as a component of speed of rotation besides inhibitor concentration at variables temperature 25, 50 and 75 °C.

All of the investigational results, computed at the 3D cubic as reported in Fig. 9, showed that it was possible to generate the corrosion rate that plummeted from 8.25 to 52.99 mL/Y. The minimum corrosion rate, 8.25 mL/Y, can be achieved at high inhibitor concentration as well as at small temperature and rotational speed levels. But at the other hand, it is likely to reach the optimum corrosion degree at low inhibitor concentration and high temperature and rotation degree rates. After all, growing inhibitor concentration results in lowering desirable corrosion rate. It is due to the **LI** inhibitor, fine established as an inhibiting

manager because it stabilizes at < 50.0 °C besides 150.0 rpm. Fig. 10 exhibits the usual plot of regression where almost all residuals fall on a horizontal path, representing the normal distribution of errors predicted. In other words, the model demonstrated better stability for predicting the response. The final equation indicated as follows in terms of the actual factors:

$$\begin{aligned}
 & * \text{Rate of corrosion (mL/Y)} = + 129.85500, \\
 & * \text{Inhibitor concentration (\%)} = - 32.47500, \\
 & * \text{Speed of rotational (rpm)} = + 0.10260, \text{ and} \\
 & * \text{Temperature (°C)} = + 0.24800.
 \end{aligned}$$

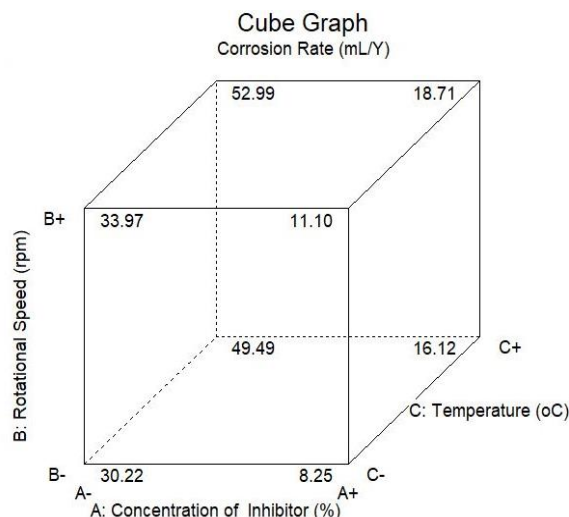


Figure 9: 3D corrosion rate plot for variables of rotational speed, inhibitor load, and temperature.

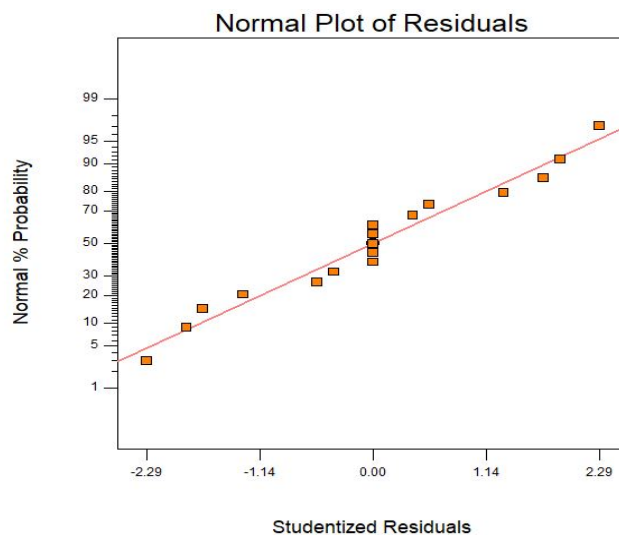


Figure 10: Standard distribution plot for the rate of corrosion error.

3.5.3. The performance of inhibitions

Fig. 11 demonstrates a contour scheme of the effect of rotational haste and concentration of inhibitor proceeding carbon steel alloy inhibition efficiency at various

temperatures of 25, 50 and 75 °C. This indicates that at 25 °C the inhibition efficiency increased between 57.89 and 86.85 % with a rising concentration of inhibitor since 5.0 to 10.0%. Increasing the rotational haste since 150.0 towards 250.0 rpm also designates no influence. Whilst also raising temperature to 50 and/or 75 °C, the efficiency of inhibition decreases with growing concentration of inhibitor and insignificant result through speed of rotation.

The contour scheme of the effect of temperature and inhibitor concentration preceding the inhibition effectiveness of carbon steel alloy at dissimilar rotational speeds of 150, 200 and 250 rpm revealed that the inhibition efficiency increased from 50.81 to 84.82 % at 150 rpm with a rise in inhibitor adsorption of 5.0 to 10.0 %. In addition, the inhibition effectiveness has no effect by raising temperature since 25.0 towards 75.0 °C. The efficiency of inhibition seems to have no result in raising the speed of rotation towards 200.0 and/or 250.0 rpm.

The contour scheme of the effect of temperature and rotational haste on the inhibition effectiveness of carbon steel alloy at dissimilar adsorptions of inhibitor 5.0, 7.5 and 10.0% showed that the inhibition effectiveness has no effect at 5.0% by increased rotational speed since 150.0 towards 250.0 rpm. Increasing concentration of inhibitors from 5 to 10% also improves inhibition performance since 45.77 towards 84.82%. The inhibition efficiency increases by increasing the concentration of inhibitors to 7.5 and/or 10%.

Fig. 12 displays the 3D scheme of carbon steel inhibition efficiency by means of a component of the inhibitor concentration and haste of rotation at various temperatures of 25, 50 and 75 °C. It indicated that the higher efficiency of inhibition was 46.37% at 25 °C. The temperature increase from 50 to 75 °C also raises the average inhibition efficiency to 43.73 and 35.09 mL/Y, accordingly.

The 3D plot of carbon steel alloy inhibition efficiency for inhibitor load and temperature at various rotational speeds of 150, 200 and 250 rpm revealed that the high inhibition efficiency was 35.84% at 150 rpm. Increasing the speed of rotation since 200.0 towards 250.0 rpm also displays that the inhibition efficiency increases towards 35.66 and 35.09%, individually.

The 3D plot of carbon steel alloy inhibition efficiency for rotation speed and temperature at variables and the relationship of inhibitors 5, 7.5 and 10% showed that the inhibition efficiency was 35.09% at 5%. Growing the temperature since 7.5 besides 10.0% also increases the extreme effectiveness of inhibition towards 69.34 besides 77.65%.

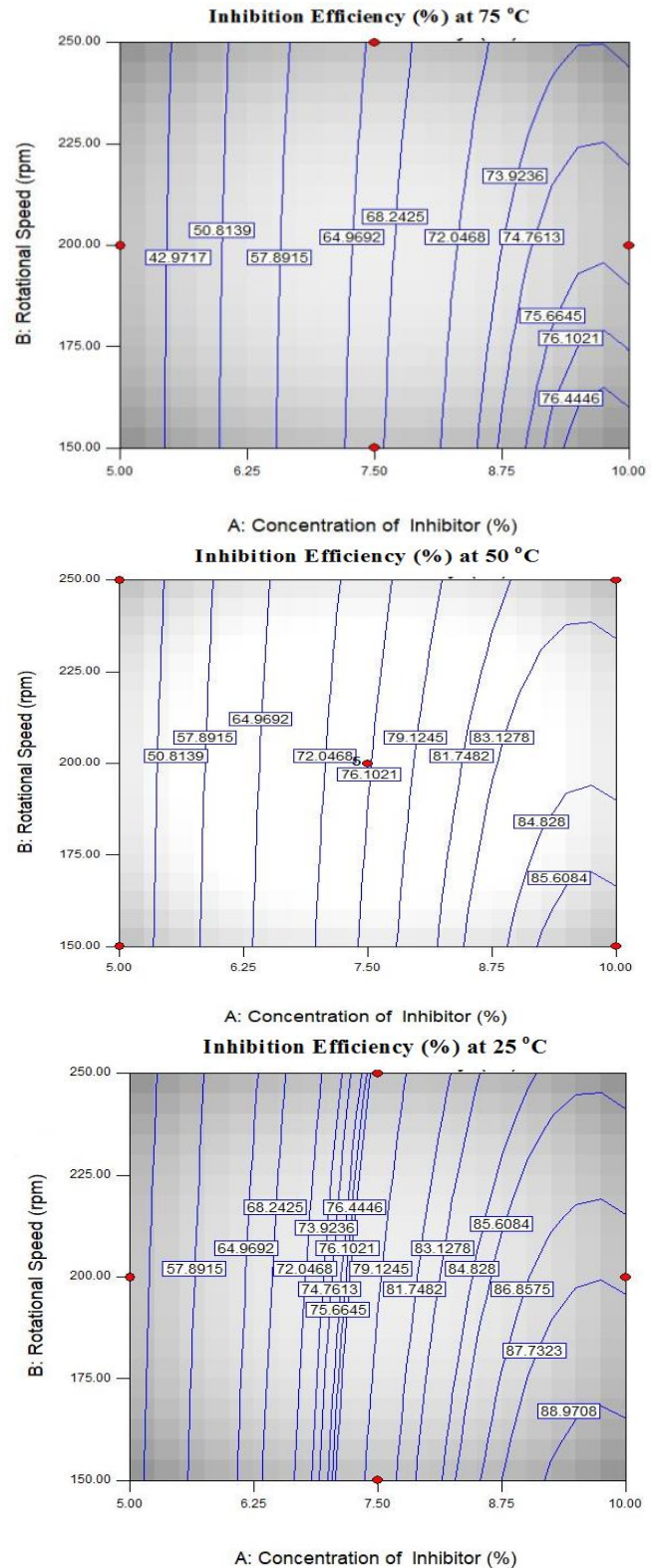


Figure 11: Contour plot of inhibition efficiency at temperatures 25, 50 and 75 °C, by means of rotational speed and inhibitor concentration.

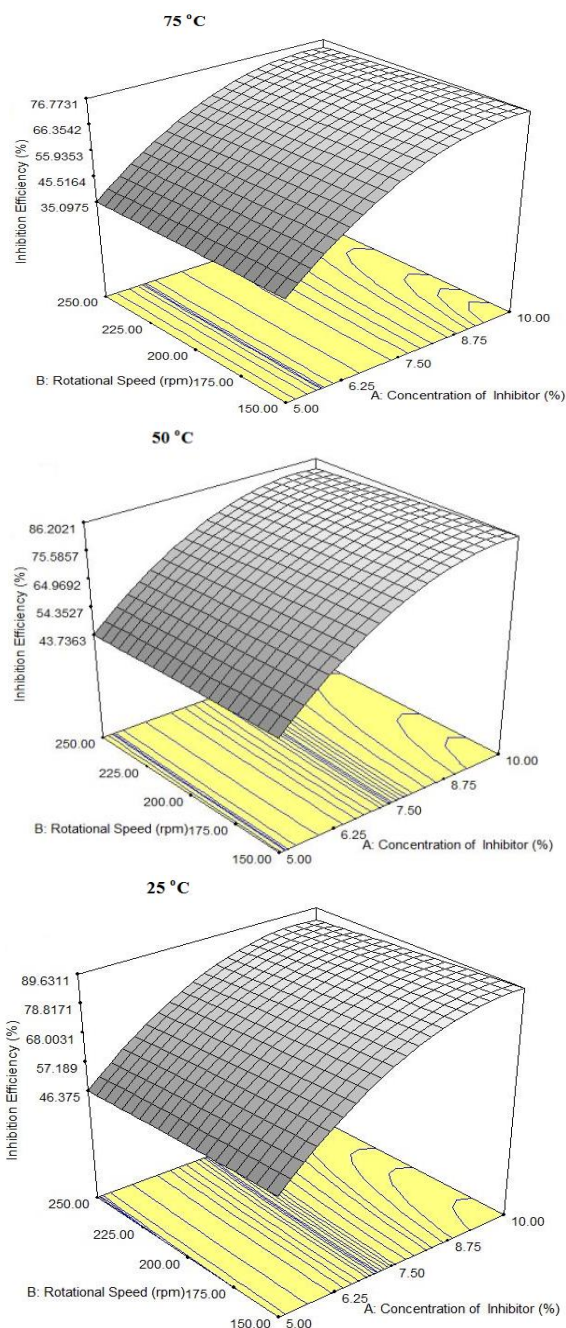


Figure 12: 3D inhibition performance plot as a meaning of the rotation speed besides inhibitor concentration by 25, 50 and 75 °C temperature.

All of the research data, consisting at the 3D-cubic as shown in Fig 13, demonstrates that the effectiveness of inhibition that plummeted from 35.10 to 89.54 % could be generated. The lowest inhibition efficiency, 35.10%, can be achieved at a small concentration of inhibitor, high temperature, and high rotational speed. At the other hand, the maximum inhibition output can be achieved at high inhibitor concentration and at low temperature and rotational speed stages [42] [43]. After all, increasing the inhibitor load leads to increased desirable inhibition efficacy. It is due to the inhibitor, fine recognized as an inhibiting manager because it stabilizes by < 50.0 °C

besides 150.0 rpm. The standard plot of residuals, representing the predicted errors to be distributed uniformly (Fig. 14). In other words, the model shows good stability for predicting the response. The final equation in terms of actual factors indicated as follows:

$$\begin{aligned} \text{Inhibition Efficiency (\%)} &= - 87.64000 \\ \text{Concentration of Inhibitor (\%)} &= + 35.98200 \\ \text{Rotational Speed (rpm)} &= + 0.025875 \\ \text{Temperature (°C)} &= + 0.18825 \end{aligned}$$

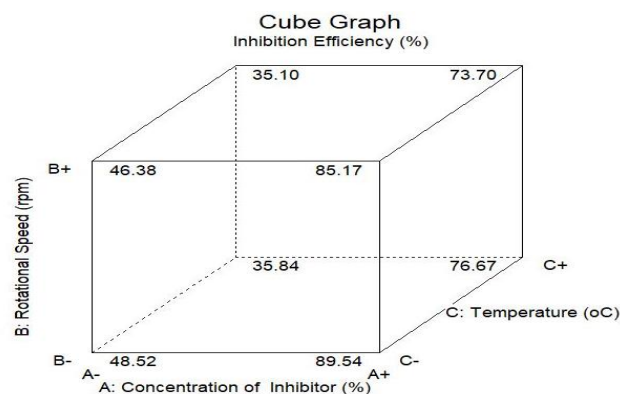


Figure 13: 3D inhibition efficiency plot for variables of rotational speed, inhibitor load, and temperature.

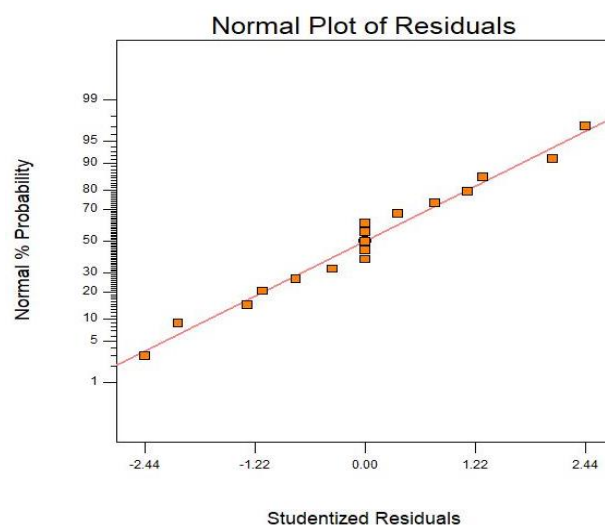


Figure 14: Standard distribution plot for the inhibition efficiency error

3.6. Mechanism of Corrosion Inhibition

The above results imply that the extract is bound to the surface of carbon steel. It is widely assumed that adsorption at the steel-solution interface would be the first stage of the inhibition process in violent saline media (Fig. 15). Several mechanisms for the adsorption of organic molecules to the steel-solution interface were suggested depending on the presence of heterocyclic atoms such as N, O and S. As it is recognized the presence of the lone pair of electrons is a

heavy inhibitor. Since, the hetero atoms improve the adsorption process and import a homogenous protective layer on the metallic surface. The previous work on the mode of action of organic compounds as a corrosion inhibitor revealed that the physical adsorption is more common compared with chemical adsorption that is because of forming more than one layer of adsorption.

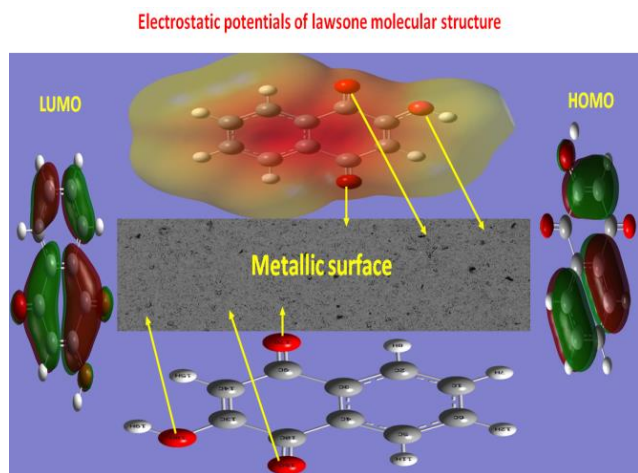


Figure 15: Corrosion inhibition mechanism of lawsone structure.

4. CONCLUSIONS

Corrosion activity and carbon steel corrosion inhibition in 3.5 wt.% NaCl electrolytes by **LI** at three different parameters such as temperature, rotational speeds and inhibitor concentrations were investigated using electrochemical techniques. These measurements designated that the increase of temperature and rotational speed increase the corrosion rate but in case of increasing the inhibitor concentrations, the corrosion rates are decreased. Both have been calculated by the growth of corrosion current and corrosion rate as well as the reduction of polarization resistance by raising the temperature and rotational speed. In case of EIS results, the carbon steel superficial and polarization resistances diminution with increasing the temperature and rotational speed owing to the incapability of carbon steel superficial to develop some rust coating under the unceasing outbreak of NaCl particles. The attendance of **LI** particles diminished the cathodic, anodic, and corrosion currents, besides deterioration rate as well as enlarged the polarization and solution resistance of the carbon steel alloy in the saline electrolyte. Inquiries into SEM and EDX are inveterate; the corrosion inhibition of carbon steel in 3.5 wt.% NaCl media is realized through the adsorption of **LI** fragments on the superficial of carbon steel alloy preventing its decomposition. The statistical analysis planned trials produced on the Box–Behnken method were castoff to evaluate the percentage of effectiveness deterioration in the presence of **LI** as inhibitor. All consequences inveterate that, the carbon steel

alloy suffers an extra corrosion with the upsurge of temperature and rotational speed in the uninhibited saline medium and that, the occurrence of **LI** and the growth of its loads diminutions the corrosion process.

Credit Authorship Contribution Statement:

Ashraf M. El-Shamy: Experimental work and analysis, **Medhat A. El-Hadek:** Reviewing & Supervision, **Ahmed E. Nassef:** Reviewing & Supervision, **Reham A. El-Bindary:** Experimental work, analysis and editing.

Declaration of Competing Interest:

The authors declare that they have no known competing financial interests or personal relationships that could have appeared to influence the work reported in this paper.

References

- [1] Pakiet, M., Kowalczyk, I. H., Leiva Garcia, R., Akid, R., and Brycki, B. E., Influence of Different Counter Ions on Gemini Surfactants with Polyamine Platform as Corrosion Inhibitors for Stainless Steel AISI 304 in 3 M HCl, *J. Mol. Liq.*, 268: 824–831, 2018.
- [2] Kaczerewska, O., Leiva-Garcia, R., Akid, R., Brycki, B., Kowalczyk, I., and Pospieszny, T., Effectiveness of Obridged cationic Gemini surfactants as Corrosion Inhibitors for Stainless Steel in 3M HCl: Experimental and theoretical studies, *J. Mol. Liq.*, 249: 1113–1124, 2018.
- [3] Alkhrafi, F. M., El-Shamy, A. M., and Ateya, B. G., Comparative Effect of Tolytriazole and Benzotriazole against Sulfide Attack on Copper, *Int. J. Electrochem. Sci.*, 4: 1351–1364, 2009.
- [4] Behzadi, H., and Forghani, A., Correlation between electronic parameters and corrosion inhibition of benzothiazole derivatives- NMR parameters as important and neglected descriptors, *J. Mol. Struct.*, 1131: 163–170, 2017.
- [5] Shehata, M. F., El-Shamy, A. M., Zohdy, K. M., Sherif, E. S. M., and Zein El Abedin, S., Studies on the antibacterial influence of two ionic liquids and their corrosion inhibition performance, *Appl. Sci.*, 10: 1444–1453, 2020.
- [6] Zohdy, K. M., El-Shamy, A. M., Kalmouch, A., and Gad, E. A. M. The corrosion inhibition of (2Z,2' Z)-4,4'-(1,2-phenylene bis(azanediy)) bis (4-oxobut-2-enoic acid) for carbon steel in acidic media using DFT, *Egypt. J. Petroleum*, 28: 355–359, 2019.
- [7] Alvarez, P. E., Fiori-Bimbi, M. V., Neske, A., Brandán, S. A., and Gervasi, C. A., Rollinia occidentalis extract as green corrosion inhibitor for carbon steel in HCl solution, *J. Ind. Eng. Chem.*, 58: 92–99, 2018.
- [8] Ateya, B. G., Alkharafi, F. M., El-Shamy, A. M., Saad, A. Y., and Abdalla, R. M., Electrochemical

- desulphurization of geothermal fluids under high temperature and pressure, *J. Appl. Electrochem.*, 39: 383–389, 2009.
- [9] Farag, A. A., Ismail, A. S., and Migahed, M. A., Environmental-friendly shrimp waste protein corrosion inhibitor for carbon steel in 1 M HCl solution, *Egypt. J. Petroleum*, 27: 1187–1194, 2018.
- [10] Shaker, M. A., and Abdel-Rahman, H. H., Corrosion of copper metal in presence of binary mixtures, *Am. J. Appl. Sci.*, 4: 554–564, 2007.
- [11] Haldhar, R., Prasad, D., and Saxena, A., Myristica fragrans extract as an eco-friendly corrosion inhibitor for mild steel in 0.5 M H₂SO₄ solution, *J. Environ. Chem. Eng.*, 6: 2290–2301, 2018.
- [12] Saxena, A., Prasad, D., Haldhar, R., Singh, G., and Kumar, A., Use of *Sida cordifolia* extract as green corrosion inhibitor for mild steel in 0.5 M H₂SO₄, *J. Environ. Chem. Eng.*, 6: 694–700, 2018.
- [13] Dehghani, A., Bahlakeh, G., and Ramezanzadeh, B. A., detailed electrochemical/theoretical exploration of the aqueous Chinese gooseberry fruit shell extract as a green and cheap corrosion inhibitor for mild steel in acidic solution, *J. Mol. Liq.*, 282: 366–384, 2019.
- [14] Bahlakeh, G., Ramezanzadeh, B., Dehghani, A., and Ramezanzadeh, M., Novel cost-effective and high performance green inhibitor based on aqueous *Peganum harmala* (Esfand) seed extract for mild steel corrosion in HCl solution: Detailed experimental and electronic/atomic level computational explorations, *J. Mol. Liq.*, 283: 174–195, 2019.
- [15] Dehghani, A., Bahlakeh, G., Ramezanzadeh, B., and Ramezanzadeh, M., Detailed macro-/micro-scale exploration of the excellent active corrosion inhibition of a novel environmentally friendly green inhibitor for carbon steel in acidic environments, *J. Taiwan Inst. Chem. Eng.*, 100: 239–261, 2019.
- [16] Sanaei, Z., Ramezanzadeh, M., Bahlakeh, G., and Ramezanzadeh, B., Use of *Rosa canina* fruit extract as a green corrosion inhibitor for mild steel in 1 M HCl solution: A complementary experimental, molecular dynamics and quantum mechanics investigation, *J. Ind. Eng. Chem.*, 69: 18–31, 2019.
- [17] Saxena, A., Prasad, D., and Haldhar, R., Investigation of corrosion inhibition effect and adsorption activities of *Cuscuta reflexa* extract for mild steel in 0.5 M H₂SO₄, *Bioelectrochem.*, 124: 156–164, 2018.
- [18] Reda, Y., El-Shamy, A. M., Zohdy, K. M., and Eessaa, A. K., Instrument of chloride ions on the pitting corrosion of electroplated steel alloy 4130, *Ain Shams Eng. J.*, 11: 191–199, 2020.
- [19] Liu, H., Fu, C., Ding, G., Fang, Y., Yun, Y., and Norra, S., Effects of hairy crab breeding on drinking water quality in a shallow lake, *Sci. Total Environ.*, 662: 48–56, 2019.
- [20] Atta, A. H., Mohamed, N. H., Nasr, S. M., and Mouneir, S. M., Phytochemical and pharmacological studies on *Convolvulus Fatmensis* Ktze, *J. Nat. Remed.*, 7: 109–119, 2007.
- [21] Sherif, E. M., Abbas, A. T., Gopi, D., and El-Shamy, A. M., Corrosion and corrosion inhibition of high strength low alloy steel in 2.0 M sulfuric acid solutions by 3-amino-1,2,3-triazole as a corrosion inhibitor, *J. Chem.*, 2014: 538794, 2014.
- [22] Sherif, E. M., Abbas, A. T., Halfa, H., and El-Shamy, A. M., Corrosion of High Strength Steel in Concentrated Sulfuric Acid Pickling Solutions and Its Inhibition by 3-Amino-5-mercapto-1,2,3-triazole, *Int. J. Electrochem. Sci.*, 10: 1777–1791, 2015.
- [23] Reda, Y., El-Shamy, A. M., and Eessaa, A. K., Effect of hydrogen embrittlement on the microstructures of electroplated steel alloy 4130, *Ain Shams Eng. J.*, 9 (4): 2973–2982, 2018.
- [24] Siebert, A., Wysocka, M., Krawczyk, B., Cholewiński, G., and Rachoń, J., Synthesis and antimicrobial activity of amino acid and peptide derivatives of mycophenolic acid, *Eur. J. Med. Chem.*, 143: 646–655, 2018.
- [25] Noll, L., Zhang, S., Wanek, W., Novel high-throughput approach to determine key processes of soil organic nitrogen cycling: Gross protein depolymerization and microbial amino acid uptake, *Soil Biol. Biochem.*, 130: 73–81, 2019.
- [26] Bailey, N., "Welding Steels without Hydrogen Cracking", Cambridge: Abington Pub., 35: 11–12, 1993.
- [27] Kr Saha, S., and Banerjee, P., Introduction of newly synthesized Schiff base molecules as efficient corrosion inhibitors for mild steel in 1 M HCl medium: an experimental, density functional theory and molecular dynamics simulation study, *Mater. Chem. Front.*, 2: 1674–1691, 2018.
- [28] Kiwaan, H. A., Atwee, T. M., Azab, E. A., and El-Bindary, A. A., Photocatalytic degradation of organic dyes in the presence of nanostructured titanium dioxide, *J. Mol. Struct.* 1200: 127115, 2020.
- [29] El-Shamy, A. M., El-Hadek, M. A., Nassef, A. E., and El-Bindary, R. A., Optimization of the Influencing Variables on the Corrosion Property of Steel Alloy 4130 in 3.5 wt.% NaCl Solution, *J. Chem.*, 2020: 9212491, 2020.
- [30] Cornell, J. A., and Montgomery, D. C., Interaction models as alternatives to low-order polynomials, *J. Qual. Technol.*, 28: 163–176, 1996.
- [31] El-Shamy, A. M., El-Hadek, M. A., Nassef, A. E., and El-Bindary, R.A., Box-Behnken design to enhance the

- corrosion resistance of high strength steel alloy in 3.5 wt.% NaCl solution, *Mor. J. Chem.* 8: XX-XX, 2020.
- [32] Saha, S. K., Ghosh, P., Hens, A., N. Murmu, C., and Banerjee, P., Density functional theory and molecular dynamics simulation study on corrosion inhibition performance of mild steel by mercapto-quinoline Schiff base corrosion inhibitor, *Phys. E.*, 66: 332–341, 2015.
- [33] Musa, A. Y., Jalgham, R. T., and Mohamad, A. B., Molecular dynamic and quantum chemical calculations for phthalazine derivatives as corrosion inhibitors of mild steel in 1M HCl, *Corros. Sci.*, 56: 176–183, 2012.
- [34] John, S., Kuruvilla, M., and Joseph, A., Adsorption and inhibition effect of methyl carbamate on copper metal in 1 N HNO₃: an experimental and theoretical study, *RSC Adv.*, 3: 8929–8938, 2013.
- [35] Ji, G., Anjum, S., Sundaram, S., and Prakash, R., Musaparadisica peel extract as green corrosion inhibitor for mild steel in HCl solution, *Corros. Sci.*, 90: 107–117, 2015.
- [36] Dutta, A., Saha, S. K., Banerjee, P., and Sukul, D., Correlating electronic structure with corrosion inhibition potentiality of some bis-benzimidazole derivatives for mild steel in hydrochloric acid: combined experimental and theoretical studies, *Corros. Sci.*, 98: 541–550, 2015.
- [37] S. D. Accelrys Software Inc., 2009.
- [38] Srivastava, V., Haque, J., Verma, C., Singh, P., Lgaz, H., Salghi, R., and Quraishi, M., Amino acid-based imidazolium zwitterions as novel and green corrosion inhibitors for mild steel: experimental, DFT and MD studies, *J. Mol. Liq.*, 244: 340–352, 2017.
- [39] Salarvand, Z., Amirnasr, M., Talebian, M., Raeissi, K., and Meghdadi, S., Enhanced corrosion resistance of mild steel in 1M HCl solution by trace amount of 2-phenylbenzothiazole derivatives: experimental, quantum chemical calculations and molecular dynamics (MD) simulation studies, *Corros. Sci.*, 114: 133–145, 2017.
- [40] Lalitha, A., Ramesh, S., and Rajeswari, S., Surface protection of copper in acid medium by azoles and surfactants, *Electrochim. Acta*, 51: 47–55, 2005.
- [41] Yeganeh, M., Asadi, N., Omid, M., and Mahdavian, M., An investigation on the corrosion behavior of the epoxy coating embedded with mesoporous silica nanocontainer loaded by sulfamethazine inhibitor, *Prog. Org. Coat.*, 128: 75–81, 2019.
- [42] Adel-Aal, E. A., El-Midany, A. A., and El-Shall, H., Mechanochemical-hydrothermal preparation of nanocrystallite hydroxyapatite using statistical design, *Mater. Chem. Phys.*, 112: 202–207, 2008.
- [43] Reda, Y., Zohdy, K. M., Eessaa, A. K., and El-Shamy, A. M., Effect of Plating Materials on the Corrosion

Properties of Steel Alloy 4130, *Egypt. J. Chem.*, 63 (2): 6–7, 2020.